In vivo clonal analysis reveals lineage-restricted progenitor characteristics in mammalian kidney development, maintenance, and regeneration

Rinkevich, Y.; Montoro, D.T.; Contreras-Trujillo, H.; Harari-Steinberg, O.; Newman, A.M.; Tsai, J.M.; Lim, X.; van Amerongen, R.; Bowman, A.; Januszyk, M.; Pleniceanu, O.; Nusse, R.; Longaker, M.T.; Weissman, I.L.; Dekel, B.

DOI
10.1016/j.celrep.2014.04.018

Publication date
2014

Document Version
Final published version

Published in
Cell Reports

OPEN ACCESS
CellPress

Cell Reports
Article

In Vivo Clonal Analysis Reveals Lineage-Restricted Progenitor Characteristics in Mammalian Kidney Development, Maintenance, and Regeneration

Yuval Rinkevich,[1,*] Daniel T. Montoro,[2] Humberto Contreras-Trujillo,[1] Orit Harari-Steinberg,[3] Aaron M. Newman,[1] Jonathan M. Tsai,[1] Xinhong Lim,[1] Renee Van-Amerongen,[1] Angela Bowman,[1] Michael Januszyk,[2] Oren Pleniceanu,[3] Roel Nusse,[1,4] Michael T. Longaker,[1,2] Irving L. Weissman,[1,5,6] and Benjamin Dekel[3,6,*]

[1]Stanford Institute for Stem Cell Biology and Regenerative Medicine, Stanford University School of Medicine, Stanford, CA 94305, USA
[2]Hagey Laboratory for Pediatric Regenerative Medicine, Department of Surgery, Plastic and Reconstructive Surgery, Stanford University School of Medicine, Stanford, CA 94305, USA
[3]Pediatric Stem Cell Research Institute, Edmond and Lily Safra Children's Hospital, Sheba Medical Center, Tel Hashomer, Sackler School of Medicine, Tel Aviv University, Tel Aviv 52621, Israel
[4]Department of Developmental Biology, Howard Hughes Medical Institute, Stanford University School of Medicine, Stanford, CA 94305, USA
[5]Ludwig Center for Cancer Stem Cell Research, Stanford University, Stanford, CA 94305, USA
[6]Co-senior author
*Correspondence: ryuval@stanford.edu (Y.R.), binyamin.dekel@sheba.health.gov.il (B.D.)
http://dx.doi.org/10.1016/j.celrep.2014.04.018

SUMMARY

The mechanism and magnitude by which the mammalian kidney generates and maintains its proximal tubules, distal tubules, and collecting ducts remain controversial. Here, we use long-term in vivo genetic lineage tracing and clonal analysis of individual cells from kidneys undergoing development, maintenance, and regeneration. We show that the adult mammalian kidney undergoes continuous tubulogenesis via expansions of fate-restricted clones. Kidneys recovering from damage undergo tubulogenesis through expansions of clones with segment-specific borders, and renal spheres developing in vitro from individual cells maintain distinct, segment-specific fates. Analysis of mice derived by transfer of color-marked embryonic stem cells (ESCs) into uncolored blastocysts demonstrates that nephrons are polyclonal, developing from expansions of singly fated clones. Finally, we show that adult renal clones are derived from Wnt-responsive precursors, and their tracing in vivo generates tubules that are segment specific. Collectively, these analyses demonstrate that fate-restricted precursors functioning as unipotent progenitors continuously maintain and self-preserve the mouse kidney throughout life.

INTRODUCTION

The adult mammalian kidney has been classically regarded as a static organ with limited cellular turnover and regenerative capacity (Little, 2006). Nephrogenesis, the process by which new nephrons are generated, initiates in a unique anatomical site of the developing kidney cortex: the cap mesenchyme (CM). In the CM, multipotent stem/progenitor cells are believed to form whole nephrons until 34 weeks of human gestation and for 1–2 weeks in the postnatal mouse, after which the nephrogenic zone exhausts its stem/progenitors (Dressler, 2009; Rosenblum, 2008; Hartman et al., 2007). Humans are estimated to be born with 300,000 to 1 million nephrons and are unable to generate additional whole nephrons under physiological or pathological conditions (Rosenblum, 2008). This is in contrast to invertebrates (Singh et al., 2007) (fly) and lower vertebrates (Diep et al., 2011) (fish), where multipotent renal stem/progenitors are thought to exist in adulthood. In the developing mouse embryo, lineage-tracing studies demonstrate that undifferentiated CM gives rise to all epithelial cell types of the adult nephron (Herzlinger et al., 1992; Kobayashi et al., 2008; Boyle et al., 2008) and that this population self-renews, fulfilling the requirements for stem cells similar to the reports from the adult fly and fish (Singh et al., 2007; Diep et al., 2011).

Although the regenerative capacity of the adult mammalian kidney remains largely unexplored at the single cell level, the appearance of epithelial cells in the urine due to normal shedding (68,000–72,000 cells/hr; Prescott, 1966) and the documented renal repair that follows damage suggest that the mammalian kidney undergoes constant cellular renewal (Little, 2006). Various cellular models for the maintenance and repair of the adult mammalian kidney have been proposed, including (1) circulating extrarenal cells (Pleniceanu et al., 2010), (2) renal epithelial cells undergoing limited and terminal cell divisions (Bonventre, 2003; Humphreys et al., 2008, 2011), and (3) multipotent adult renal stem cells (Oliver et al., 2004; Bussolati et al., 2005; Sagrinati et al., 2006; Dekel et al., 2006; Maeshima et al., 2006; Appel et al., 2009).

As such, a fundamental question in renal biology still exists as to how and to what extent the kidney physiologically maintains and regenerates its entire compartments in vivo. We utilized

long-term genetic lineage tracing and clonal analysis of individual cells to analyze the magnitude of tissue renewal within the adult mammalian kidney and to discriminate between the proposed cellular modes. Our results reveal a mechanism of continuous regeneration and cellular renewal of kidney epithelia by fate-restricted and segment-specific clones, beginning from fetal stage and persisting throughout adult life.

RESULTS AND DISCUSSION

Clonal Analysis in the Adult Kidney

Mouse kidneys continue to grow in mass for the first 12 weeks postparturition (from 8 to 12 weeks; $p = 0.001046$), a time point from which they maintain a steady-state mass (Figure 1A; from 12 to 40 weeks; $p = 0.208876$). These values were used to establish periods in which renal growth was absent and in which the magnitude and cellular mechanisms underlying renal maintenance could be assessed.

We genetically lineage traced individual cells within the adult kidney (>12 weeks) using "Rainbow" mice (Rinkevich et al., 2011), which harbor a multicolor (red, yellow, green, and blue) Cre-dependent reporter construct within the ROSA locus ($R26^{VT2/GK3}$). To analyze all renal epithelial cell types, including rare and presumed multipotent stem cells, we employed a lineage-tracing strategy that was independent of candidate markers by crossing Rainbow mice with mice harboring an inducible Cre-ER fusion protein under the ubiquitous Actin promoter ($Actin^{CreER}$). $Actin^{CreER}$; $R26^{VT2/GK3}$ offspring were injected with tamoxifen at 12 weeks of age to induce cytoplasmic fusion protein to enter the nucleus and randomly recombine permanently a single color-encoding gene. Mice were sacrificed following 1, 2, 4, and 7 months, at which times the fluorescent patterns were analyzed. Over a 1-month period, small two to three epithelial cell clones were scattered throughout the cortex, medullae, and papillae (Figure S1A, 1 month, n = 400). Over extended periods, a subset of epithelial cells increased in size over time, giving rise to large (more than eight cells) clones that have contributed substantially to existing tubules within the cortex (Figure 1B, dotted white line), medulla (Figure 1C, dotted white line), and papillae (Figure 1D).

Each single color segment was uninterrupted by any single cell of another color, ruling out migration of other cells into the clonal region. In each time point (1, 2, 4, and 7 months), only epithelial cell types were in the clone, indicating that physiological epithelial-mesenchymal transformation (EMT) is not apparent within the kidney (Duffield and Humphreys, 2011; Duffield, 2010). These results are not consistent with interstitial mesenchymal cells contributing to renal epithelial repair (Humphreys et al., 2008, 2010) but are consistent with intrinsic renal epithelial cells that mediate tubulogenesis. To rule out the possibility of cellular contributions from adjacent and similarly colored cells to these clones, we performed genetic lineage tracing by administering single and low doses of tamoxifen (see the Experimental Procedures). In these experiments, the frequency of recombination was low (<1%) such that renal epithelial cells were sparsely labeled within large and noncolored kidney domains. Despite the scarcity of labeled cells, kidneys subjected to lineage tracing over 7 months showed single-colored and large clones of 10–12 cells in all kidney regions (Figures 1E–1G), highlighting genuine clonal outputs by individual cells.

To visualize the full sizes and distributions of clones, we isolated intact nephron segments (Schafer et al., 1997) from $Actin^{CreER}$; $R26^{VT2/GK3}$ mice that were chased for 7 months. Intact tubules either showed no significant tubulogenesis in some instances (Figure 1H) or contained large epithelial clones (Figures 1I and 1J) within individual segments (n = 75), consistent with epifluorescence analysis of serial sections. Large clones of more than ten cells expanded along the longitudinal and perpendicular axes of tubules (Figures 1I and 1J), contributing circumferentially as well as longitudinally to tubule segments. These results indicate that substantial tubulogenesis has occurred within the adult renal epithelium. Despite the lack of increase in renal mass from 12 weeks postparturition onward (Figure 1A), cumulative counting of cell divisions (see the Experimental Procedures) in the adult kidney over 7 months indicated that the magnitude of tubulogenesis within the adult kidney is equivalent to 4.6–6 times complete renewal of the renal epithelium (×4.6, cortex; ×6, medullae; ×5, papillae). Tissue renewal occurred despite 20%–25% of renal epithelial cells failing to divide, indicating that only a subset of adult epithelial cells generates new tubule segments postnatally.

The composition of new tubule segments generated postnatally by renal clones was determined by using distinguishing markers for the various tubule types (Laitinen et al., 1987) (Figure 2A; see the Experimental Procedures). A total of 31 clones were examined within convoluted distal tubules (DTs) and stained entirely with DT-specific marker peanut agglutinin (PNA) in the mouse cortex (Figures 2B–2B‴). A total of 54 clones were examined within convoluted proximal tubules (PTs) and stained entirely with the PT-specific marker lotus tetragonolobus lectin (LTA) (Figures 2F–2F‴ and 2G–2G‴), whereas 115 clones examined within the collecting ducts (CDs) stained entirely for CD-specific markers aquaporin 2 (AQP2) and aquaporin 3 (AQP3) in the mouse papilla (Figures 2C–2C‴ and 2D–2D‴). Indeed, combinations of single and double staining using LTA/Mucin 1 (MUC1) (Figures 2E–2E‴), LTA/PNA (Figures 2F–2F‴), and LTA/Calbindin (Figures 2G–2G‴) indicated that clones maintained composition of a single renal lineage and tubule type, including clones (n = 200) at the interface between tubule segments (Figures S1B–S1B‴, S1C–S1C‴, and S1D–S1D‴). Given the complete absence of clonal expansion into different segments on the scale of these experiments, it is likely that the clone-initiating cells that maintain constant tubulogenesis within the adult kidney are intrinsically limited in their capacity for differentiation and that a multipotent stem cell, if at all present, is physiologically negligible to adult tissue renewal. We did not costain MUC1 and PNA because MUC1 also expresses to a certain extent in distal convoluted tubules, and therefore this staining could not definitely discriminate segment-specific clones.

Negligible Contributions from Circulating Cells to Kidney Maintenance

To address the possibility of a circulating population of cells that contribute to adult tubulogenesis, we generated pairs of genetically marked parabiotic mice that have a shared anastomosed circulatory system (Wagers et al., 2002). Wild-type mice were

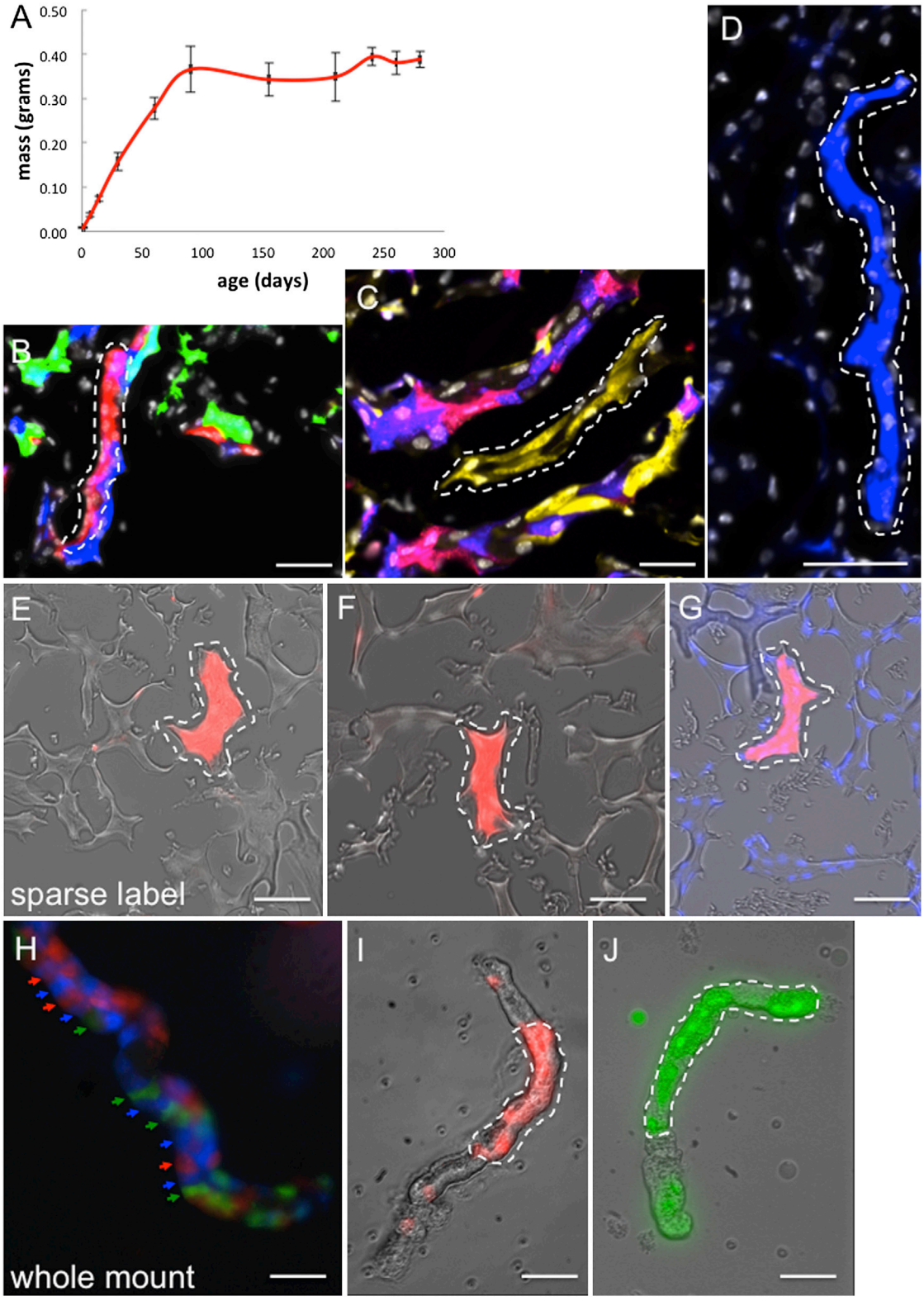

Figure 1. Clonal Analysis during Adult Kidney Growth

(A) Line chart depicting the mean change in kidney mass over time. x axis represents age in days. y axis represents kidney mass in grams.

(B–D) Composite (Rainbow and DAPI) images from *Actin*^{CreER}; *R26*$^{VT2/GK3}$ mice that were chased for 7 months. Singly colored clones contribute to distinct segments in the renal cortex (B, single red clone is outlined), medulla (C, single yellow clone is outlined), and papilla (D, blue clone is outlined).

(legend continued on next page)

surgically conjoined to mice expressing GFP under a ubiquitous (chicken β-actin) promoter. These mice develop full hematopoietic chimerism within a month (Wagers et al., 2002). Kidneys from wild-type mice that were removed after 12 months of parabiosis showed donor-derived GFP^+ cells throughout interstitial spaces of the kidney, in the renal pelvis, and in cell foci surrounding some glomeruli (Figure S2) that did not incorporate into any glomerular, tubular, vascular, or epithelial structures, or express endothelial or renal epithelial markers (Figure S2). All GFP^+ cells expressed the pan hematopoietic marker CD45 (Figures S2 and S2D–S2D″) as well as CD11c and F4/80 (Figures S2, S2E–S2E″, and S2F–S2F″), indicating that they belong to the monocyte/macrophage lineage. We found no evidence of contributions from circulating cells, of any type, to cell turnover within the kidney, including glomerular mesangium, which was previously suggested to repopulate from bone marrow cells (Cornacchia et al., 2001).

These results of renal tubule-restricted clonal segment-specific epithelial cells are complemented by our previous studies that demonstrated generation of nonepithelial fibroblasts and smooth muscle cells from a mesothelial precursor lineage (Rinkevich et al., 2012) and collectively demonstrate a mechanism of organ renewal by tissue- and lineage-restricted precursors for both renal tubule and nontubule (endothelial, smooth muscle, mesothelium, and fibroblast) components. Like our studies on digit-tip regeneration in mice, wherein lineage-restricted local tissue-type-specific stem/progenitor cells (Rinkevich et al., 2012) rather than dedifferentiated pluripotent blastema cells are responsible for regeneration, and our previous studies that blood-forming stem cells can only make blood (Wagers et al., 2002), and not other tissues such as heart cells (Balsam et al., 2004), brain cells (Massengale et al., 2005), or any endoderm-derived epithelial cells (Wagers and Weissman, 2004) by transdifferentiation, it appears that the mouse and human body plans for tissue maintenance occurs via tissue-restricted and tissue subregion-specific cells with stem/progenitor characteristics.

Clonal Analysis of the Developing Kidney

During kidney development, early mesenchyme of the nephrogenic cortex is induced to undergo mesenchymal-epithelial transition (MET) and differentiates into kidney epithelium (Dressler, 2009; Rosenblum, 2008; Harari-Steinberg et al., 2013). In the pre-MET developmental stage, Six2 specifies mesenchymal progenitors that can give rise to multiple cell types of the nephron tubule (Kobayashi et al., 2008). Post-MET developmental stages represent induced epithelia at varying stages of differentiation and mature nephron tubules. We performed clonal analysis of renal tubules at post-MET stages to identify cellular mechanisms of tubule growth.

Using the $Actin^{CreER}$; $R26^{VT2/GK3}$ system, we traced embryonic renal progenitors from gestational stage of embryonic day 13.5 (E13.5) up to postnatal day 1 (P1) (see Experimental Procedures). In these post-MET stages, tubules were polyclonal, derived from multiple mixed progenitors (Figures 3B–3D, dotted white lines) similar to lineage-tracing observations of adult kidneys. We separately generated tetrachimeric mice by injecting mouse embryonic stem cells (mESCs) that stably express separate fluorescent proteins (GFP-mESCs), red fluorescent protein (RFP-mESCs), and cyan fluorescent protein (CFP-mESCs) into wild-type blastocysts (Ueno and Weissman, 2006). Within tetrachimera kidneys, mature nephrons were polyclonal, revealing mixed contributions of clones to individual tubule segments (Figures 3E–3H). A similar polyclonal pattern was observed under confocal fluorescent microscopy in both renal tubules (Figure 3I) and glomeruli (Figures 3J–3J″). Within the renal papilla, we found a pattern of clonal foci (Y.R., unpublished data), indicating that their progenitors directly seed the renal papilla without prior cellular intermixing. This mosaic polyclonal composition of kidney epithelia (both in CM-derived nephron epithelia and CDs derived from ureteric buds) suggests that several types of stem/progenitor cells are present during kidney organogenesis. Immunostaining for renal epithelial subtypes in tetrachimeras illustrated that clones were separately composed of PT, DT, or CD fates (Figures 3K–3P). Thus, whereas the in vivo clonal analysis cannot definitely assess the pre-MET stage, it indicates that similar to adulthood, at least during the post-MET developmental stages, the immediate contributing precursors to the kidney tubules are locally restricted to a single lineage and tubule type.

Clonal Analysis of the Kidney during Repair

We investigated the response of the kidney to acute injury by performing unilateral ischemia/reperfusion (I/R) to the left kidneys of adult mice (Bonventre and Yang, 2011). Kidneys subjected to I/R showed extensive tubular damage characterized by loss of the epithelial brush border (Figure S3B, black asterisk), flattening of epithelial cells, necrotic tubular cells, and tubular casts at 72 hr postinjury (Figure S3B, black arrowheads). At 4 days postinjury, trichrome-stained kidney sections revealed ectopic collagen deposition and interstitial fibrosis (Figure S3D), especially in those kidneys subjected to prolonged occlusion times (60 and 75 min). To investigate the clonal responses of the kidney to renal injury, tamoxifen was injected into $Actin^{CreER}$; $R26^{VT2/GK3}$ mice, followed by clamping of the left renal arteries. Kidneys were harvested and sectioned after 2 months to allow the cumulative representations of all potential clones (early and late) triggered during the injury response, including cell activities involved in physiologic renal maintenance during this period. Single colored clones appeared in the damaged kidney cortex (Figures 4A–4A″, dotted white lines), medulla (Figures 4B–4B″, dotted white lines), and papilla (Figures 4C–4C″, dotted white lines) and were restricted to their nascent tubule segments of PTs, DTs, and CDs. In areas of damage, we found significant tubulogenesis (Figures 4B and 4C), with clones that have

(E–G) Composite images from $Actin^{CreER}$; $R26^{VT2/GK3}$ mice following a low-dose regimen of tamoxifen, showing single and sparse clones of eight to ten cells (E–G, dotted white line).
(H–J) Isolated nephron segments from $Actin^{CreER}$; $R26^{VT2/GK3}$ mice that were chased for 7 months reveal that some tubule segments lack any clonal expansions (H, arrows), whereas others show extensive tubulogenesis by single colored clones (I and J, dotted white line).
Scale bars represent 50 μm (B–D and H–J) and 25 μm (E–G).

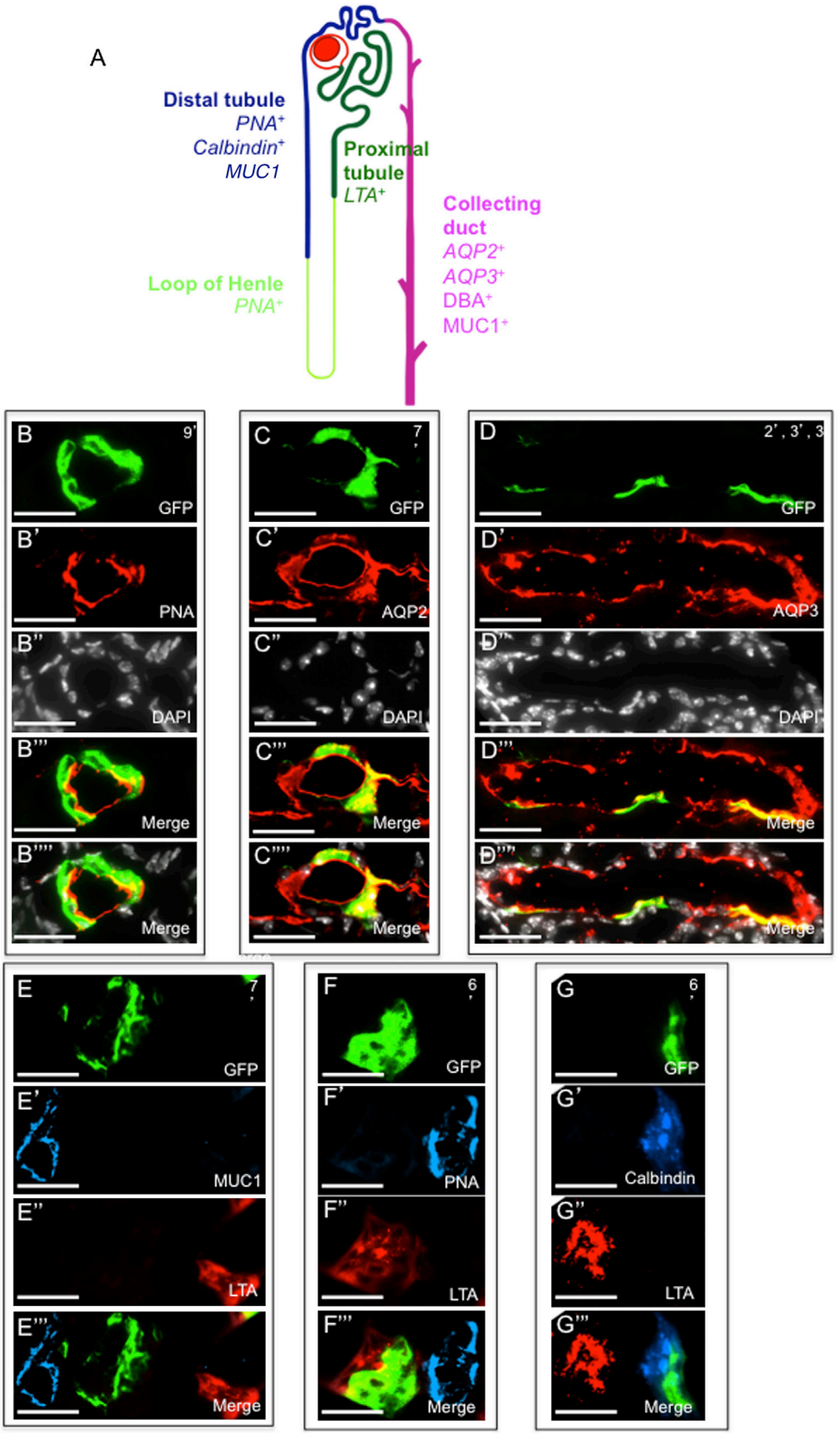

(legend on next page)

contributed circumferentially to an entire tubule. Confocal and epifluorescence analyses of serial sections indicated that clones expanded in parallel to the longitudinal and perpendicular axes of a tubule (Figures 4D and 4D′) but that did not cross to adjacent segments within a nephron (on the transverse plane) nor to neighboring nephrons (on the sagittal plane). Quantitative counting of clones indicated that significantly more epithelial cells entered cell cycle following injury than did during maintenance, with the highest surge of cell division occurring in the renal cortex (60% versus 41%, Figure S4A).

The possibility of a multipotent cell phenotype emerging in response to damage was determined by analyzing the long-term fates of renal clones. Clones within I/R-subjected kidneys were entirely retained within the domain of a single tubule marker (or completely absent; Figures 4E–4E‴, 4F–4F‴, and 4G–4G‴). Double immunostaining of dolichos biflorus agglutinin (DBA)/LTA (Figures 4H–4H‴) and AQ3/LTA (Figures 4I–4I‴) in areas of renal damage confirmed that clones maintained the fate of one single renal lineage and tubule type, similar to adult maintenance and fetal development.

We explored a second model of acute renal failure using intramuscular injection of glycerol (Figures S3 and S3E–S3H), which results in rhabdomyolysis and myoglobinuria leading to toxic tubular damage (Buzhor et al., 2013). Significant tubulogenesis was independently observed in kidneys that were acutely subjected to glycerol-induced injury (Figure S5) and by expansions of clonal precursors that are fate restricted (Figures S5F and S5G).

Establishment of Renal Organoids In Vitro

To investigate the in vitro fates from individual renal precursors, we established a culture system of growing renal epithelial organoids in suspension (Ootani et al., 2009; Buzhor et al., 2011) (see the Experimental Procedures). Kidneys were harvested from *Actin*^{CreER}; *R26*$^{VT2/GK3}$ mice following tamoxifen injection, dissociated into single cells, and plated with Matrigel on 24- and 48-well plates. Within several days of culturing, multiple renal organoids developed, gradually enlarged, and then opened into hollow spheres resembling renal tubes in vivo. We found that monoclonal, biclonal, and polyclonal spheres emerged in our culture systems (Figures 5A–5A‴) with similar propensity, appearance, and size.

To test the in vitro clonal efficiency of renal progenitors, we plated *Actin*^{CreER}; *R26*$^{VT2/GK3}$ renal cells in limiting dilution. Approximately 30, 6, and 1 spheres emerged per well following the culture of 1×10^6, 1×10^5, and 1×10^4 cells, respectively (average formation of spheres/well was 1.4 spheres/10,000 cells or 0.014%, Figure 5C). Within all dilutions, a similar propensity for monoclonal/polyclonal spheres emerged (43%/57% in 1×10^6 cells, 50%/50% in 1×10^5 cells, and 52%/48% in 1×10^4 cells), indicating that progenitor frequency, not aggregations between renal cells, most likely underlies the frequency of renal spheres expanded in our culture system. Serial passaging of renal spheres over three sequential passages (Figure 5D) revealed that monoclonal spheres are constantly formed, and with increased propensity over time, which is consistent with a subset of cells with self-renewal potential. We then analyzed the fate of monoclonal renal spheres derived from individual cells by staining with antibodies to distinct renal tubule segments. For each segment-specific marker we tested, spheres either stained entirely within all epithelial cells (Figures 5E–5E‴ and 5F–5F‴) or were entirely absent of label (n = 48). Double and triple staining using combinations of segment-specific markers revealed that each renal sphere is fate restricted to one tubule segment only (Figures 5G–5G‴, 5H–5H‴, and 5I–5I‴), indicating that renal precursors give rise in vitro to epithelial descendants of the same tubule type (PTs, DTs, and CDs). Although our culture conditions support all developmental fates, and spheres in serial passages, we cannot exclude the possibility that the culture conditions biased against a multipotent fate, an increasingly unlikely possibility given the concordance of our in vivo and in vitro data presented here.

Clonal Analysis of Wnt-Responsive Cells

To examine renal precursors' response to Wnt signaling, we analyzed the expression of Axin2 (Conductin) protein, a gene whose transcription is induced by β-catenin that has translocated into the nucleus and that provides negative feedback in the Wnt-β-catenin signaling pathway (Lustig et al., 2002). Kidneys from *Axin2*^{lacz} transgenic mice, which express LacZ protein under the control of the endogenous *Axin2* promoter/enhancer region, showed expression in single cells within the collecting system and the PTs (Figures 6A and 6A′). We then lineage traced the fate of single Wnt-responding cells (WRCs) using mice harboring an inducible Cre-ER under the promoter of the *Axin2* gene (van Amerongen et al., 2012) (*Axin2*^{CreER}). *Axin2*^{CreER} transgenic mice were crossed with *R26*^{mTmG}, a double-fluorescent reporter mouse that replaces the expression of tomato red with GFP after Cre-mediated excision (Muzumdar et al., 2007). Kidneys from *Axin2*^{CreER}; *R26*^{mTmG} (double-heterozygote) offspring showed GFP expression within single cells of the collecting system, and PTs 4 days after tamoxifen injection, similar to the pattern observed in *Axin2*^{lacz} transgenic mice (Figure 6A″). Single WRCs that were traced from gestational stage E17.5 up to the

Figure 2. Fate Restriction of Clones during Adult Kidney Maintenance

(A) Illustration of a single nephron tubule with DT, loop of Henle, PT, and CD segments. Segment-specific markers (provided in the image) were used to characterize the composition of individually colored clones.

(B–D) Long-lived clones that emerge following 7 months of chase are entirely retained within the segment-specific domains of label.

(B) PNA$^+$ illustrates a clone with a DT fate.

(C and D) AQP2 and AQP3 illustrate clones with a CD fate.

(E–G) Double immunostaining of segment-specific markers shows that clones are fate restricted to a single tubule type.

(E) LTA$^-$ MUC1$^-$ illustrates a clone with a non-PT/non-CD most likely DT fate.

(F) LTA$^+$ PNA$^-$ illustrates a clone with a PT fate.

(G) Calbindin$^+$ LTA$^-$ illustrates a clone with DT fate.

In (B)–(G), numbers on top right-hand side of images represent the clone size. Scale bars represent 50 μm (B–G).

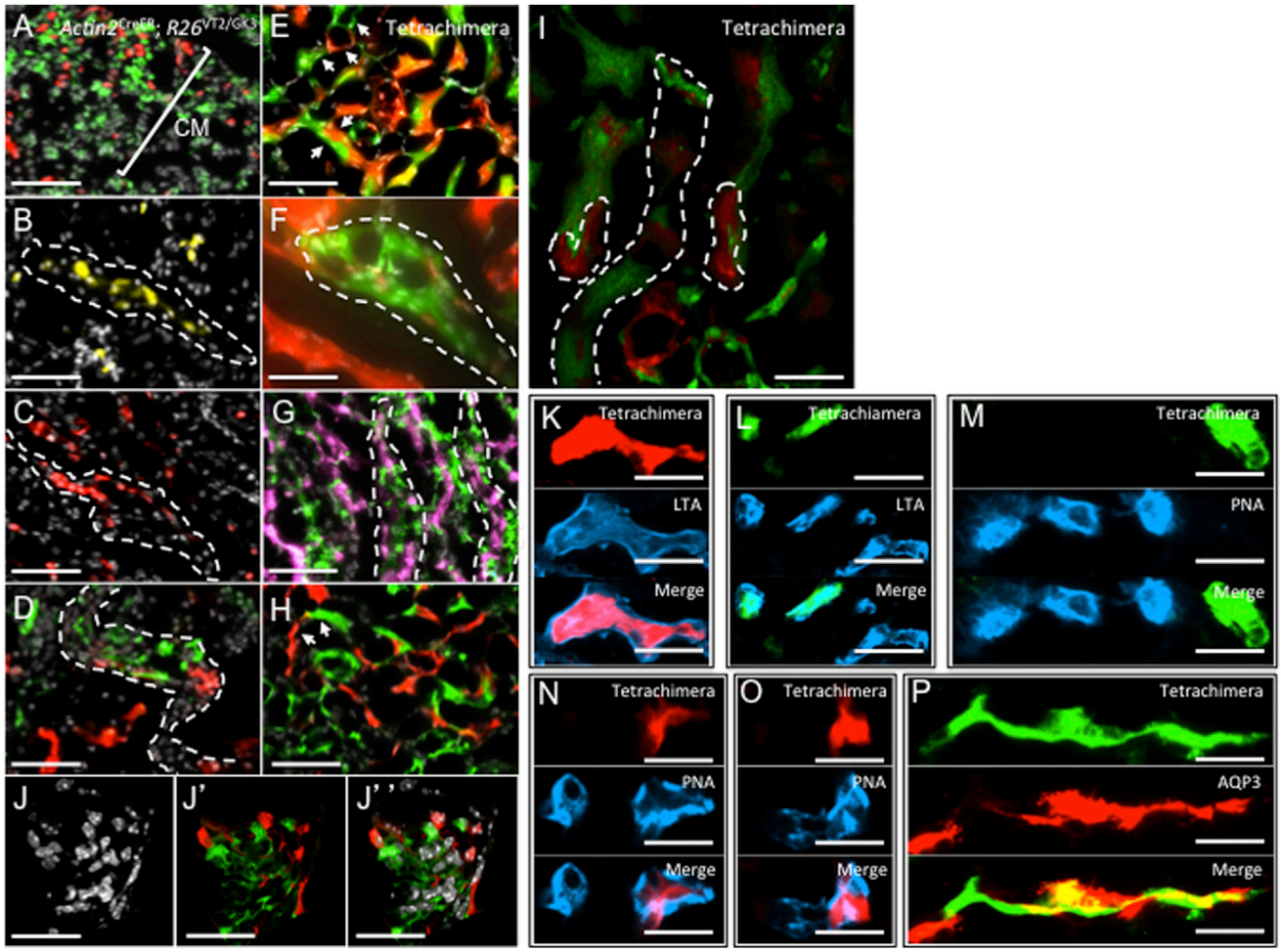

Figure 3. Clonal Analysis of the Developing Kidney

(A–D) Composite images (Rainbow and DAPI) from *Actin*^{CreER}; *R26*$^{VT2/GK3}$ mice that were traced from gestational stage of E13.5 up to P1.

(A) Lineage-traced cells in the CM are intermixed at the cortex prior to differentiation (white line).

(B and C) At post-MET stages, tubules are expanding from mixed progenitors (dotted white line) creating the future polyclonal nephrons.

(D) A later stage in a developing tubule shows separate red and green clones contributing to a single tubule segment.

(E–H) Composite (Rainbow and DAPI) images of renal tubules from a tetrachimeric mouse.

(E) An image of the medulla showing polyclonal nephron and CD tubules. White arrows indicate boarders between clones within individual nephrons.

(F) High-power image showing nondividing cells (white arrows) and cell processes interspersed within a green clone. Dotted white line indicates the boarder of the green clone within adjacent and separately colored tubule.

(G and H) Separately colored clones are retained within tubules of the CD.

(I and J–J″) Confocal fluorescent microscopy image of the medulla and a glomerular mesangium showing separate red and green clones of mesangial cells.

(K–P) Singly colored clones from tetrachimeric mice are fate restricted to PTs (K–M, LTA$^+$ PNA$^-$), DT (N and O, PNA$^+$), or CD fates (P, AQP3$^+$).

Scale bars represent 50 μm (I–P) and 25 μm (A–H).

third postnatal month showed large GFP$^+$ clones within the cortex that were developmentally restricted to a PT fate (Figures 6B and 6B′). Separate GFP$^+$ clones appeared within the medullary papilla that were developmentally restricted to a CD fate (Figures 6B″ and 6B‴). Isolation of intact nephron segments from *Axin2*^{CreER}; *R26*^{mTmG} mice indicated that single WRCs regenerated new tubule segments (Figures 6C–6C″, 6D–6D″, and 6E–6E″), with more than a single tubule segment renewing per PT (Figures 6C″, 6D″, and 6E″). A similar fate restriction of clones was documented in kidneys from *Axin2*^{CreER} mice crossed to "Rainbow" reporter mice (*Axin2*^{CreER}; *R26*$^{VT2/GK3}$) that were lineage traced from E17.5 up to the fifth postnatal month. In these kidneys, single WRCs contributed separate colored clones to CD or PT fates (Figures 6F–6F‴). We then counted the clone sizes that emerged in *Axin2*^{CreER}; *R26*$^{VT2/GK3}$ kidneys (n = 1,580) and found that 97% of all WRCs (at the time of tamoxifen injection) formed large clones of up to 11 cells (Figure 6G). This represents a substantial increase in the proliferative capacity of WRCs compared to non-Wnt-distinguished cells, with the distribution of the former resembling the upper 5% of the latter.

Immunostaining of single WRC-derived clones for segment-specific markers showed that clones were restricted to either a

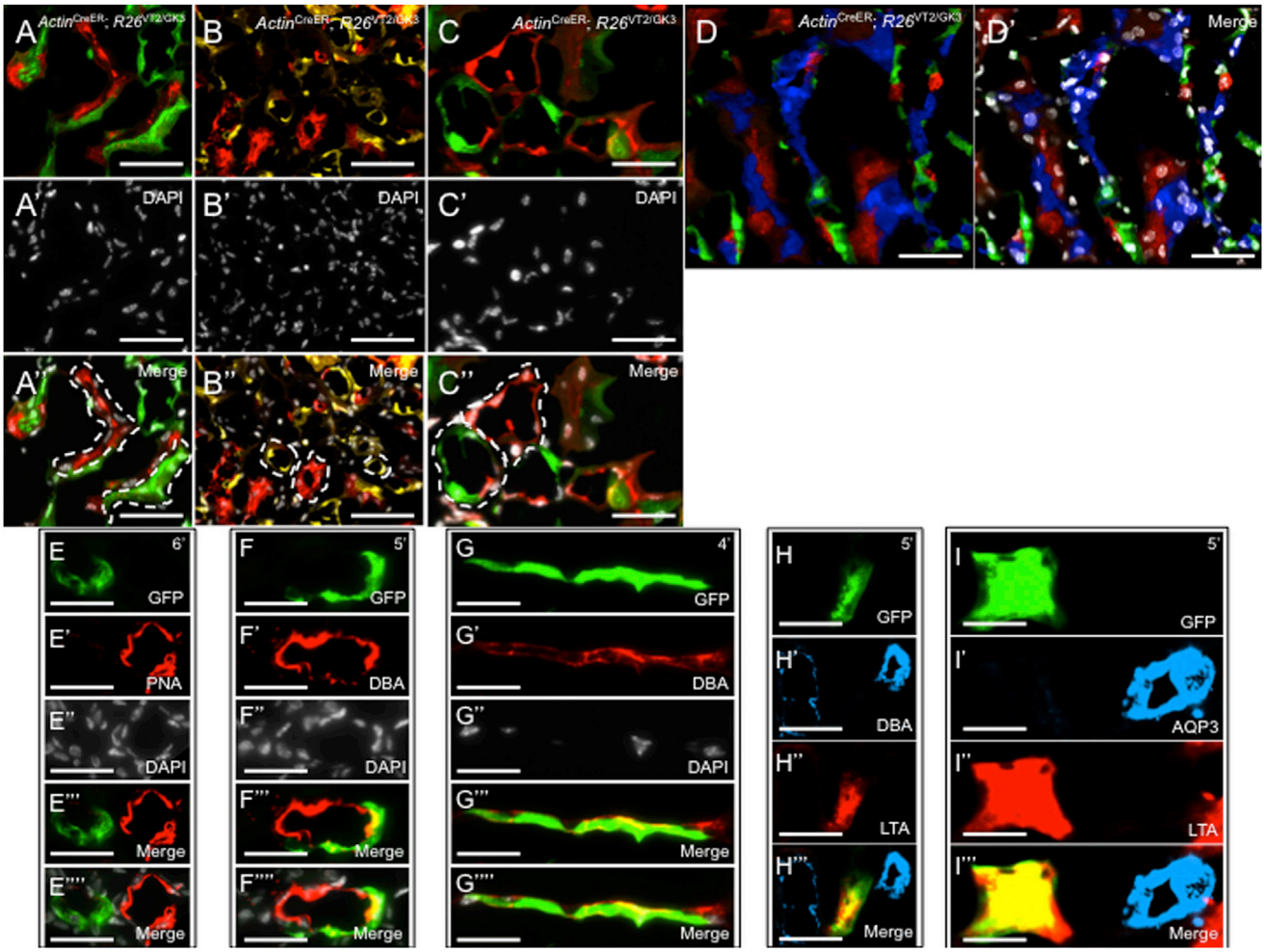

Figure 4. Clonal Analysis of the Mammalian Kidney following I/R

(A–C) Composite Rainbow images from *Actin*^{CreER}; *R26*$^{VT2/GK3}$ mice following 2 months of tracing.

(A–A″) Singly colored red and green clones contributing to the damaged renal cortex.

(B–B″) Singly colored yellow and red clones contributing to the damaged renal medulla.

(C–C″) High-power image showing red and green clones contributing to the damaged CDs.

(D and D′) Confocal Rainbow images of the renal medulla showing that clones are retained within segments following renal damage.

(E–I) Singly colored clones that emerge following renal damage are fate restricted. Clones are either completely absent (PNA$^-$ for non-DT fate, E–E‴′) or entirely express (DBA$^+$ for CD fate, F–F‴′ and G–G‴′) the segment-specific markers. Double immunostaining of segment-specific markers shows a green clone that is LTA$^+$ DBA$^-$ (H) and LTA$^+$ AQP3$^-$ (I) both representing a PT fate.

Scale bars represent 50 μm (A and C–I) and 25 μm (B).

PT or CD fate. Within the renal cortex, clones were LTA$^+$ (Figures 6H–6H‴′) and PNA$^-$ (Figures 6I–6I‴′), consistent with a PT fate. Within the renal papilla, clones were DBA$^+$ (Figures 6J–6J‴′), AQP2$^+$ (Figures 6K–6K‴′), and AQP3$^+$ (Figures 6L–6L‴′), consistent with a CD fate.

We then analyzed the contributions of WRCs to tubulogenesis that follows acute renal failure, using intramuscular injection of glycerol (Figure S6). After 2 months, *Axin2*^{CreER}; *R26*^{mTmG} mice (n = 3) that were subjected to glycerol-induced damage revealed predominantly (95%) large clones that contributed new tubule segments within PTs (Figures S6A–S6A″) and CDs (Figures S6B–S6B″ and S6C–S6C″). Lineage tracing of individual Axin2$^+$ cells in a similar manner using the *Axin2*^{CreER}; *R26*$^{VT2/GK3}$ system (n = 3) revealed single-colored and large clones within the renal epithelium and that significant tubulogenesis has occurred via single Axin2$^+$ precursors within PTs (Figures S6D–S6D″) and CDs (Figures S6E–S6E″). These observations are consistent with the subsets of cells with highest proliferative capacity observed using the *Actin*^{CreER} system. The fact that Axin2 is expressed (at the time of recombination) within a subset of renal epithelial cells, that then trace long-lived and large clones of up to 11 cells, suggests that the molecular phenotype of the clone-forming cells is distinct from those of their daughter cells and is consistent with a stem cell and/or progenitor characteristic of proximal and collecting system tubules. Going beyond the scope of this manuscript, it would be interesting

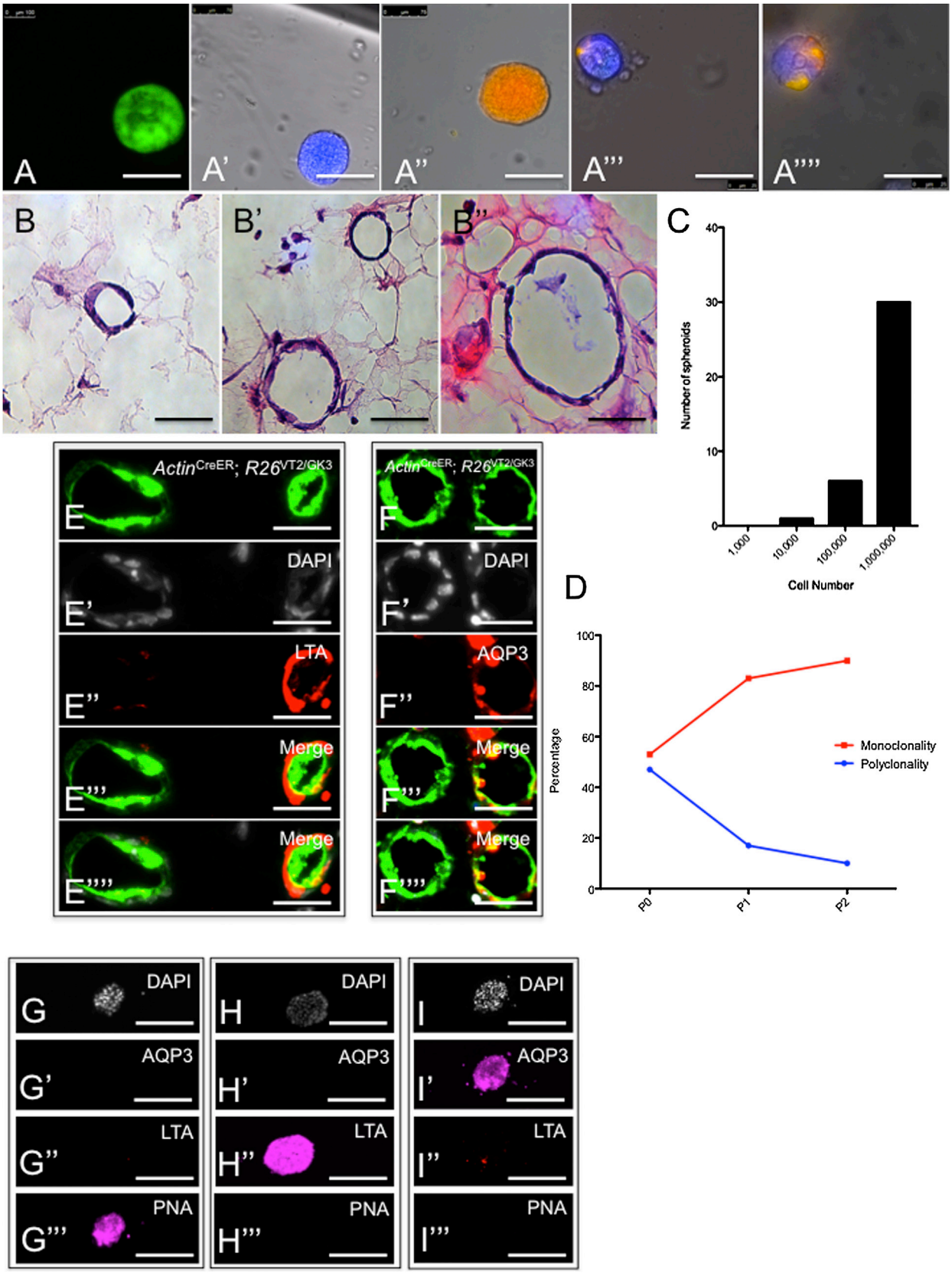

(legend on next page)

to assess whether WRCs are a predetermined subset or represent a transient step of cell differentiation induced by local Wnt stimuli.

A recent report by Barker et al. (2012) has identified LGR5$^+$ cells as the immediate progenitors that generate the thick ascending limb of Henle's loop and distal convoluted tubule during kidney development. Although LGR5, itself a Wnt-responsive gene, is silenced at later postnatal stages of development and fails to trace clone-forming cells in the adult, our analysis demonstrates that constant tubulogenesis is occurring within the mammalian kidney via a similar mechanism involving fate-restricted precursors throughout physiologic renal maintenance and following regeneration-induced damage. During the revision stages of this manuscript, two publications described fate mapping of PT epithelia during renal injury: Kusaba et al. (2014) and Berger et al. (2014). Different from our long-term and unbiased clonal analysis regimen, these groups use marker genes to follow the fates of PT epithelia and independently demonstrate that expanding PT epithelia are fate restricted in their development during renal injury.

Thus, the daily shedding of epithelial cells from all compartments into the urine (Prescott, 1966) can be replenished by local cell production from Wnt-responsive, fate-restricted, and clone-forming cells that may function as unipotent stem/progenitor cells. It is possible that the scattered distribution of single WRCs indicates that they are self-renewed and, thus, are unipotential stem cells, but a more formal analysis of this possibility requires further study.

This mechanism could equally explain the compensatory renal growth that has been documented following nephrectomy (Kaufman et al., 1975) and the idiopathic renal growth documented in pediatric patients with either solitary or single-functioning kidneys (Spira et al., 2009). It also serves to explain the restricted fates and subtypes that have been observed within renal cell carcinomas (Valladares Ayerbes et al., 2008) and inherited kidney disorders (Klootwijk et al., 2014; Bockenhauer et al., 2009) arising from specific kidney segments.

These experiments emphasize the importance of using genetic labeling of individual cells. Histological/immunohistochemical data (Witzgall et al., 1994), staining patterns of bromodeoxyuridine label retention by cells (Oliver et al., 2004), or experiments where multiple thymidine analogs have been pulsed then chased (Humphreys et al., 2008) would greatly depend on previous knowledge of the cell-cycle kinetics of resident cells. Without that knowledge, the distinction between a slow-cycling progenitor and a differentiated cell undergoing its last cell division could not be made.

A similar cellular framework may also take place in liver and pancreas, where self-duplications of adult pancreatic islet cells (Dor et al., 2004) and liver hepatocytes have been reported. In those organs, as in the kidney, a morphologically homogeneous population can nevertheless contain clonogenic subsets, here shown to be the Wnt-responsive cells, that produce the fate-restricted kidney epithelial cells, display enhanced proliferative capacity, as well as retain the low frequency of WRCs, therefore offering a therapeutic target to increase or restore the regenerative capacity of the mammalian kidney.

EXPERIMENTAL PROCEDURES

Mice

Mice were derived and maintained at the Stanford University Research Animal Facility in accordance with Stanford University guidelines. All the animals were housed in sterile microinsulators and given water and rodent chow ad libitum. *Actin*^{CreER} transgenic mice were a gift from Dr. Liqun Luo (Stanford University). *Axin2*^{lacZ} and *Axin2*^{CreER} (The Jackson Laboratory; strain name B6.129(Cg)-*Axin2*$^{tm1(cre/ERT2)Rnu}$/J, stock number 018867) were a gift from Dr. Roel Nusse (Stanford University). *R26*$^{mT/mG}$ transgenic mice were obtained from The Jackson Laboratory (strain name B6.129(Cg)-Gt(ROSA) 26Sor < tm4(ACTB-tdTomato,-EGFP); strain number 007676). Male mice were used in all experiments, unless stated otherwise. Parabiosed wild-type mice were all females.

Mice Genotyping

The following primers and PCR conditions were used for genotyping:

Cre: 5′-CGGTCGATGCAACGAGTGATGAGG-3′ and 5′-CCAGAGACGGAA ATCCATCGCTCG-3′; 94°C for 10 min, 94°C for 30 s, 56°C for 1:30 min, and 72°C for 1:30 min; and repeat 35 cycles, 72°C for 8 min.

mTmG: 5′-CTCTGCTGCCTCCTGGCTTCT-3′, 5′-CGAGGCGGATCACAAG CAATA-3′, and 5′-TCAATGGGCGGGGGTCGTT-3′; 94°C for 3 min, 94°C for 30 s, 61°C for 1 min, and 72°C for 1 min; and repeat 35 cycles, 72°C for 2 min.

Tamoxifen Injections

Male mice were used in all experiments, unless stated otherwise. All strains used for genetic lineage tracing (including *Actin*^{CreER}; *R26*^{Rainbow} and *Axin*^{CreER}; *R26*^{mTmG}) were assessed for leakiness in adult kidneys and show negative Rainbow fluorescence (using *R26*^{Rainbow} reporter) or GFP (using *R26*^{mTmG} reporter) in the absence of tamoxifen administration.

Tamoxifen (Sigma-Aldrich) was prepared by dissolving in corn oil (Sigma-Aldrich) to a concentration of 20 mg/ml. A total of 4–6 mg tamoxifen was injected intraperitoneally (i.p.) every other day for 1 week, using a tuberculin syringe and 25G needle.

To find tamoxifen concentrations where sparse labeling would take place within the renal epithelium, we injected male mice at >2.5 months of age with a single dose of tamoxifen/corn oil at various concentrations. At these postnatal stages, we found that injecting tamoxifen i.p. at concentrations bellow 1 mg (n = 5 mice) does not lead to recombination within the renal cortex and medullae, but only in papillary epithelium. A dose of 1–2 mg

Figure 5. Renal Spheres that Develop from Individual Cells Are Lineage Restricted In Vitro

(A–A‴) Composite fluorescent images of spheres from single-cell suspensions of *Actin*^{CreER}; *R26*$^{VT2/GK3}$ kidneys.

(B–B″) Representative sections of renal spheres stained with hematoxylin and eosin.

(C) Histogram that graphically represents the frequency of spheres formed from cells cultured in limited dilution.

(D) Graphical representation of the frequency of monoclonal/polyclonal spheres emerging after serial passaging. Following three passages, most emerging spheres are monoclonal (red line), and not polyclonal (blue line).

(E and F) Images of sections from renal spheres immunostained with antibodies to distinct renal segments reveal that each segment-specific marker stains some but not all spheres.

(G–I) Immunostaining of three representative spheres with antibodies for segment-specific markers. Each renal sphere is fate restricted to DTs (PNA$^+$), PTs (LTA$^+$), or CDs (AQP3$^+$).

Scale bars represent 50 μm (A–A‴, B–B″, and E–I).

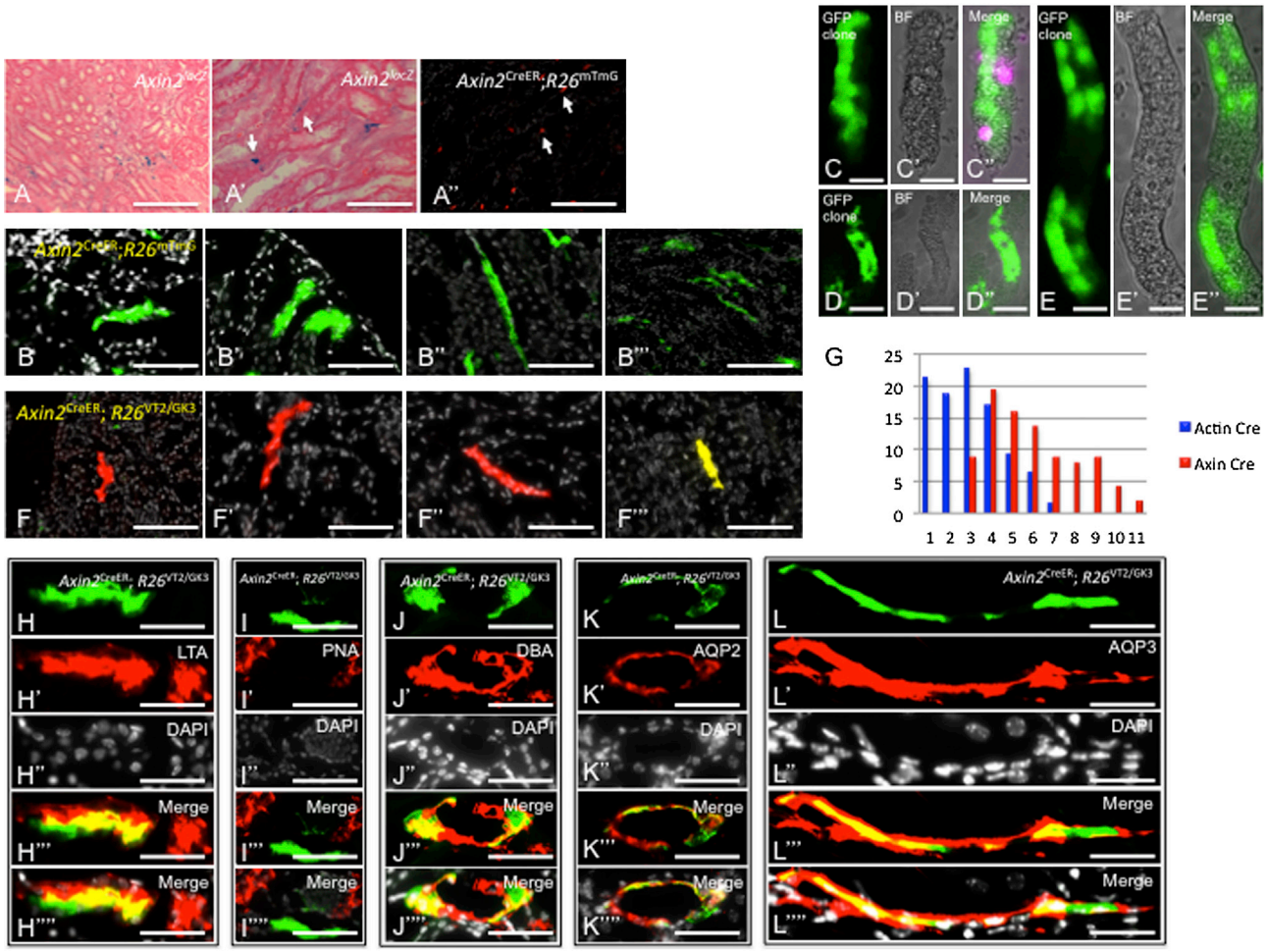

Figure 6. WRCs Are Clone-Forming Cells and Lineage Restricted In Vivo

(A and A′) Sections from *Axin*$^{lacZ/lacZ}$ kidneys stained with β-galactosidase and counterstained with eosin showing Axin2 expression within the collecting system and PTs. (A″, white arrows) *Axin2*^{CreER};*R26*^{mTmG} kidneys that were pulsed for 4 days show GFP expression within the collecting system and PTs.

(B–B‴) *Axin2*^{CreER};*R26*^{mTmG} kidneys that were pulsed from E17.5 up to the third postnatal month show large GFP^{+} clones within PTs and CDs.

(C–D) Intact PT segments from *Axin2*^{CreER};*R26*^{mTmG} kidneys show large GFP^{+} clones confined to individual segments.

(E and F) Clones derived from WRCs are lineage restricted to either PT or CD fates. Within the cortex, clones are LTA^{+}, PNA^{-} indicating PT fate.

(F–F‴) *Axin2*^{CreER}; *R26*$^{VT2/GK3}$ kidneys that were pulsed from E17.5 up to the fifth postnatal month show singly colored large clones within PTs (F and F′) and CDs (F″ and F‴).

(G) Histogram that graphically represents the difference in clonal outcomes of all cells (blue) versus WRCs (red).

(H–H‴″ and I–I‴″) Within the renal papilla, clones are DBA^{+}, AQP2^{+}, AQP3^{+} indicating CD fate (J–J‴″, K–K‴″, and L–L‴″).

Scale bars represent 50 μm (A) and 25 μm (A′, A″, B–F, and H–L).

tamoxifen/corn oil was found to be the minimal concentration where sparse labeling of around 1% would take place within all renal epithelium (n = 5).

Lineage Tracing of Embryonic Kidney

Adult female *R26*^{Rainbow} mice older than 2 months of age were mated with adult *Axin*^{CreER} or *Actin*^{CreER} males. Plugs were checked every morning, and 0.25 mg/25 g of tamoxifen diluted in corn oil was injected i.p. at days E10.5–E13.5 with a Becton Dickinson 1 ml insulin syringe with a 27G needle. Eight neonatal pups were sacked at day 1, fixed in 2% paraformaldehyde overnight, and set in optimal cutting temperature compound (OCT). Kidneys (n = 16) were subjected to 5 μm sections and analyzed for multicolor fluorescence.

Generation of Tetrachimera Mice

C57BL/6J female mice (Jackson Laboratory; strain/000664) were superovulated with 5 IU of pregnant mare serum gonadotropin (Sigma-Aldrich; G4877) and 5 IU of human chorionic gonadotropin (Sigma-Aldrich; CG 10) and mated by a standard protocol. Morulas were collected at E2.5 and cultured with EmbryoMax KSOM (Millipore; MR-106-D) overnight to blasts. For each blastocyst, a mixture of 15 ESCs was injected. For single-cell injection, Rosa-EGFP, Rosa-ECFP, and Rosa-mRFP1 ESC clones were put in a separate place on an injection chamber, and each one of the three clones was picked up and injected into a blastocyst. Injected blastocysts were then transferred into the uterus of day 2.5 pseudopregnant CD1 mice (Charles River Laboratories; #022) and allowed to reach postnatal stages of development, at which time five tetrachimera mice (male and female) were sacrificed at 30 days postparturition, and their kidneys (n = 10) were analyzed.

Renal I/R Injury

A left peritoneal incision was performed on five male mice 6–8 weeks of age to expose the kidney, followed by clamping of the left renal pedicle for 30–75 min.

Glycerol-Induced Acute Kidney Injury

Following 22 hr of water deprivation, five male mice 6–10 weeks of age received an intramuscular injection of 6–8 mg/kg hypertonic glycerol (50% v/v; Sigma-Aldrich) as divided doses in both the hindlimbs. Blood samples were collected from the retro-orbital sinus. Mice serum was extracted using 0.8 ml MiniCollect Tube (Greiner Bio-One) according to manufacturer's instructions, and blood levels of creatinine and urea were measured using the Olympus AU2700 analyzer. Blood urea nitrogen (BUN) equals urea (mg/dl) divided by 2.14.

Mice exposed to a single intramuscular injection of glycerol showed a significant rise in BUN and creatinine following 3 days (Figures S3E and S3F), which was associated with tubular epithelial injury and generalized disorganization of the normal kidney structures, including necrosis, cast formation (hyaline and cellular), and desegregation of tubular membranes (Figure S7). Clonal analysis of kidneys following 2 months showed that 40%, 38%, and 36% of renal epithelial cells entered cell cycle within the cortex, medulla, and papilla, respectively (Figure S5E). The I/R-induced clonal response is significantly different from that of the glycerol-induced response and may be an outcome of regional susceptibility to hypoxia that exists between the compartments of the kidney.

Histology and Tissue Analysis

For fixation, kidney samples were placed in 2% paraformaldehyde for 12–16 hr at 4°C and then prepared for embedding by soaking in 30% sucrose in PBS at 4°C for 24 hr. Kidney samples were removed from the sucrose solution, and tissue blocks were prepared by embedding in Tissue-Tek O.C.T. (Sakura Finetek) under dry ice to freeze the samples within the compound. Frozen blocks were mounted on a Microm HM550 cryostat (MICROM International), and 5- to 8- or 12-μm-thick sections were transferred to Superfrost Plus Adhesive Slides (Fisherbrand).

Hematoxylin and Eosin Staining

All histological stains were carried out on 8 μM formalin-fixed paraffin-embedded sections. Nuclei were stained with Gill's hematoxylin, blued with diluted ammonium hydroxide, and the cytoplasm was counterstained with acidified eosin.

Trichrome Staining

Trichrome stains of kidney samples 4 days after I/R injury were carried out according to Masson's method. Samples were deparaffinized and rehydrated, refixed in Boiun's solution, and stained with Weigert's iron hematoxylin to stain nuclei, Biebrich scarlet-acid fuchsin to stain cytoplasm and keratin, and aniline blue to stain collagen fibers.

Periodic Acid-Schiff Staining

Periodic Acid-Schiff (PAS) stains of kidney samples 3 days after glycerol administration were carried out using PAS kit (Sigma-Aldrich) according to the instructions of the manufacturer.

Confocal Microscopy

Confocal microscopy was carried out on 8–12 μM cryosections counterstained with Hoechst 33342. A Leica SP2 AOBS (Acousto-Optical Beam Splitters) confocal laser-scanning microscope was used to capture images allowing spectral detection and unmixing of overlapping spectrum with 20×, 40×, and 63× oil objectives. For resolution of nuclei-dense regions, z stacked confocal images were rendered into three dimensions using Volocity 6.0.1 software for clonal analysis.

Immunohistochemistry

Immunostaining was performed using the following primary antibodies: CD31 (Abcam), CD90 (eBioscience), PEA (BD PharMingen), Cytokeratin 5 (Abcam), Cytokeratin 14 (Covance), CD45 (BioLegend), LTA (Covance), DBA (Covance), PNA (Covance), AQP3 (Abcam), and MUC1 (Abcam). LTA immunostains PTs, PNA, and *Calbindin*, immunostain DTs, AQP2, AQP3, DBA, and MUC1 immunostain CDs.

Briefly, slides were blocked for 30 min in 10% BSA with 2% goat serum followed by incubation with primary antibody for 12–16 hr. For immunoassaying on sections from $Actin^{CreER}$; $R26^{VT2/GK3}$ mice, Alexa Fluor 647-conjugated antibody was used as secondary 1:1,000 for 1 hr (Invitrogen) and was visualized in the far-red channel (Cy5). Fluorescent and bright-field images were taken with a Leica DM4000B microscope (Leica Microsystems) and RETIGA 2000R camera (QImaging Scientific Cameras).

Cell Counting

Clones were visualized using a Leica DM4000B microscope. For each experiment, 400 clones from the renal cortex, medulla, and papilla were counted separately and then averaged. Clone size was established by incorporating the number of nuclei in each clone per section and by incorporating the total clone sizes from serial sections.

Physiological tissue renewal over 1 year was approximated by counting clones in the renal epithelium, only, and in areas with recombination frequency >95%. Overall cell division within a field was calculated by estimating the percentage of cells in each clone size times the number of cell divisions required to reach each clone size. For example, 20% of renal epithelial cells exhibiting an average clone size of ten cells/clone would indicate renewal of 20% × 9 = 180%. These values do not take into account renal epithelial cell death and shedding and, therefore, represent a lower estimation.

In Vitro Culture of Renal Cells

To isolate renal cells, adult $Actin^{CreER}$; $R26^{VT2/GK3}$ (Rainbow) mice were injected i.p. with 4–6 mg of tamoxifen (Sigma-Aldrich). Kidneys were then collected and mechanically and enzymatically dissociated in Medium 199 containing Liberase TM, TH enzymes (Roche), and DNase (Worthington) treated at 37°C until a single cell suspension was achieved. Dissociated cells were washed with PBS and serially filtered through 70 and 40 μm cell strainers. Red blood cells were lysed using ACK Lysing Buffer (Invitrogen). Single-cell suspensions were mixed with 25 μl of ice-cold Matrigel (reduced growth factors; BD Biosciences), plated in 48-well plates, and allowed to solidify at 37°C. After polymerization of Matrigel, 250 μl of culture medium was added: advanced Dulbecco's modified Eagle's medium/F12 supplemented with penicillin/streptomycin, 10 mM HEPES, GlutaMAX, 1× N2, 1× B27-A (Invitrogen), and N-acetylcysteine (Sigma-Aldrich) containing growth factors (50 ng/ml epidermal growth factor [PeproTech], 500 ng/ml R-spondin-1 [R&D Systems], and 100 ng/ml Noggin [PeproTech]). Growth factors were added every fourth day, and the entire medium was changed every 8 days.

Kidney Weight

Various aged CD-1 wild-type mice (sharing background with $Actin^{CreER}$; $R26^{VT2/GK3}$ experimental animals) were purchased from Jackson Laboratory as individuals from separate litters to control for variable husbandry and litter conditions. Left and right kidneys were collected, and mesothelium was removed for accurate weighing in triplicate on a Mettler-Toledo AB54-S/FACT Electronic Analytical Balance to the nearest 10^{-4} g. Control kidneys perfused with saline prior to weighing tended to be heavier than raw processed kidneys but did not show a significant difference between kidneys of the same weight, nor did it change the trend of kidney mass over time. Statistics between individual age groups was determined with two-tailed t test; each time point had 10–20 kidneys.

SUPPLEMENTAL INFORMATION

Supplemental Information includes six figures and can be found with this article online at http://dx.doi.org/10.1016/j.celrep.2014.04.018.

AUTHOR CONTRIBUTIONS

Y.R. and B.D. designed and performed the kidney experiments with suggestions from I.L.W. and R.N. Y.R. imaged and analyzed the data from all kidney experiments. D.T.M. performed the confocal imaging and assisted with experiments and collection and analysis of data. H.C.-T. developed, performed, and analyzed the in vitro assays. O.H.-S. analyzed outcomes of renal damage. R.V.-A. and X.L. performed the lineage tracing in $Axin^{CreER}R26^{mTmG}$ mice.

A.M.N., M.J., and Y.R. performed the statistical analysis. Y.R., D.T.M., I.L.W., M.T.L., and B.D. wrote the manuscript.

ACKNOWLEDGMENTS

We thank Adriane Mosley for assistance with animal care and parabiosis experiments and Charlene Wang for making the tetrachimeric mice. We thank Kitty Lee and the Cell Sciences Imaging Facility Fluorescent Microscopy Core at Stanford University for technical assistance with confocal microscopy. This work was supported in part by a grant from the California Institute of Regenerative Medicine (RC1 00354) and the Smith Family Trust (to I.L.W.), the Oak Foundation and the Hagey Laboratory for Pediatric Regenerative Medicine (to M.T.L.), the Israel Scientific Foundation (910-11), Israel Cancer Research Fund (PG-27013), and the Feldman Family Visiting Professorship, Stanford School of Medicine (to B.D.). Y.R. was supported by the Human Frontier Science Program Long-Term Fellowship, the Machiah Foundation Fellowship, and the Siebel foundation (1119368-104-GHBJI).

Received: July 7, 2013
Revised: March 2, 2014
Accepted: April 9, 2014
Published: May 15, 2014

REFERENCES

Appel, D., Kershaw, D.B., Smeets, B., Yuan, G., Fuss, A., Frye, B., Elger, M., Kriz, W., Floege, J., and Moeller, M.J. (2009). Recruitment of podocytes from glomerular parietal epithelial cells. J. Am. Soc. Nephrol. *20*, 333–343.

Balsam, L.B., Wagers, A.J., Christensen, J.L., Kofidis, T., Weissman, I.L., and Robbins, R.C. (2004). Haematopoietic stem cells adopt mature haematopoietic fates in ischaemic myocardium. Nature *428*, 668–673.

Barker, N., Rookmaaker, M.B., Kujala, P., Ng, A., Leushacke, M., Snippert, H., van de Wetering, M., Tan, S., Van Es, J.H., Huch, M., et al. (2012). Lgr5(+ve) stem/progenitor cells contribute to nephron formation during kidney development. Cell Rep *2*, 540–552.

Berger, K., Bangen, J.M., Hammerich, L., Liedtke, C., Floege, J., Smeets, B., and Moeller, M.J. (2014). Origin of regenerating tubular cells after acute kidney injury. Proc. Natl. Acad. Sci. USA *111*, 1533–1538.

Bockenhauer, D., Feather, S., Stanescu, H.C., Bandulik, S., Zdebik, A.A., Reichold, M., Tobin, J., Lieberer, E., Sterner, C., Landoure, G., et al. (2009). Epilepsy, ataxia, sensorineural deafness, tubulopathy, and KCNJ10 mutations. N. Engl. J. Med. *360*, 1960–1970.

Bonventre, J.V. (2003). Dedifferentiation and proliferation of surviving epithelial cells in acute renal failure. J. Am. Soc. Nephrol. *14* (*Suppl 1*), S55–S61.

Bonventre, J.V., and Yang, L. (2011). Cellular pathophysiology of ischemic acute kidney injury. J. Clin. Invest. *121*, 4210–4221.

Boyle, S., Misfeldt, A., Chandler, K.J., Deal, K.K., Southard-Smith, E.M., Mortlock, D.P., Baldwin, H.S., and de Caestecker, M. (2008). Fate mapping using Cited1-CreERT2 mice demonstrates that the cap mesenchyme contains self-renewing progenitor cells and gives rise exclusively to nephronic epithelia. Dev. Biol. *313*, 234–245.

Bussolati, B., Bruno, S., Grange, C., Buttiglieri, S., Deregibus, M.C., Cantino, D., and Camussi, G. (2005). Isolation of renal progenitor cells from adult human kidney. Am. J. Pathol. *166*, 545–555.

Buzhor, E., Harari-Steinberg, O., Omer, D., Metsuyanim, S., Jacob-Hirsch, J., Noiman, T., Dotan, Z., Goldstein, R.S., and Dekel, B. (2011). Kidney spheroids recapitulate tubular organoids leading to enhanced tubulogenic potency of human kidney-derived cells. Tissue Eng. Part A *17*, 2305–2319.

Buzhor, E., Omer, D., Harari-Steinberg, O., Dotan, Z., Vax, E., Pri-Chen, S., Metsuyanim, S., Pleniceanu, O., Goldstein, R.S., and Dekel, B. (2013). Reactivation of NCAM1 defines a subpopulation of human adult kidney epithelial cells with clonogenic and stem/progenitor properties. Am. J. Pathol. *183*, 1621–1633.

Cornacchia, F., Fornoni, A., Plati, A.R., Thomas, A., Wang, Y., Inverardi, L., Striker, L.J., and Striker, G.E. (2001). Glomerulosclerosis is transmitted by bone marrow-derived mesangial cell progenitors. J. Clin. Invest. *108*, 1649–1656.

Dekel, B., Zangi, L., Shezen, E., Reich-Zeliger, S., Eventov-Friedman, S., Katchman, H., Jacob-Hirsch, J., Amariglio, N., Rechavi, G., Margalit, R., and Reisner, Y. (2006). Isolation and characterization of nontubular sca-1+lin- multipotent stem/progenitor cells from adult mouse kidney. J. Am. Soc. Nephrol. *17*, 3300–3314.

Diep, C.Q., Ma, D., Deo, R.C., Holm, T.M., Naylor, R.W., Arora, N., Wingert, R.A., Bollig, F., Djordjevic, G., Lichman, B., et al. (2011). Identification of adult nephron progenitors capable of kidney regeneration in zebrafish. Nature *470*, 95–100.

Dor, Y., Brown, J., Martinez, O.I., and Melton, D.A. (2004). Adult pancreatic beta-cells are formed by self-duplication rather than stem-cell differentiation. Nature *429*, 41–46.

Dressler, G.R. (2009). Advances in early kidney specification, development and patterning. Development *136*, 3863–3874.

Duffield, J.S. (2010). Epithelial to mesenchymal transition in injury of solid organs: fact or artifact? Gastroenterology *139*, 1081–1083, e1–e5.

Duffield, J.S., and Humphreys, B.D. (2011). Origin of new cells in the adult kidney: results from genetic labeling techniques. Kidney Int. *79*, 494–501.

Harari-Steinberg, O., Metsuyanim, S., Omer, D., Gnatek, Y., Gershon, R., Pri-Chen, S., Ozdemir, D.D., Lerenthal, Y., Noiman, T., Ben-Hur, H., et al. (2013). Identification of human nephron progenitors capable of generation of kidney structures and functional repair of chronic renal disease. EMBO Mol Med *5*, 1556–1568.

Hartman, H.A., Lai, H.L., and Patterson, L.T. (2007). Cessation of renal morphogenesis in mice. Dev. Biol. *310*, 379–387.

Herzlinger, D., Koseki, C., Mikawa, T., and al-Awqati, Q. (1992). Metanephric mesenchyme contains multipotent stem cells whose fate is restricted after induction. Development *114*, 565–572.

Humphreys, B.D., Valerius, M.T., Kobayashi, A., Mugford, J.W., Soeung, S., Duffield, J.S., McMahon, A.P., and Bonventre, J.V. (2008). Intrinsic epithelial cells repair the kidney after injury. Cell Stem Cell *2*, 284–291.

Humphreys, B.D., Lin, S.L., Kobayashi, A., Hudson, T.E., Nowlin, B.T., Bonventre, J.V., Valerius, M.T., McMahon, A.P., and Duffield, J.S. (2010). Fate tracing reveals the pericyte and not epithelial origin of myofibroblasts in kidney fibrosis. Am. J. Pathol. *176*, 85–97.

Humphreys, B.D., Czerniak, S., DiRocco, D.P., Hasnain, W., Cheema, R., and Bonventre, J.V. (2011). Repair of injured proximal tubule does not involve specialized progenitors. Proc. Natl. Acad. Sci. USA *108*, 9226–9231.

Kaufman, J.M., Hardy, R., and Hayslett, J.P. (1975). Age-dependent characteristics of compensatory renal growth. Kidney Int. *8*, 21–26.

Klootwijk, E.D., Reichold, M., Helip-Wooley, A., Tolaymat, A., Broeker, C., Robinette, S.L., Reinders, J., Peindl, D., Renner, K., Eberhart, K., et al. (2014). Mistargeting of peroxisomal EHHADH and inherited renal Fanconi's syndrome. N. Engl. J. Med. *370*, 129–138.

Kobayashi, A., Valerius, M.T., Mugford, J.W., Carroll, T.J., Self, M., Oliver, G., and McMahon, A.P. (2008). Six2 defines and regulates a multipotent self-renewing nephron progenitor population throughout mammalian kidney development. Cell Stem Cell *3*, 169–181.

Kusaba, T., Lalli, M., Kramann, R., Kobayashi, A., and Humphreys, B.D. (2014). Differentiated kidney epithelial cells repair injured proximal tubule. Proc. Natl. Acad. Sci. USA *111*, 1527–1532.

Laitinen, L., Virtanen, I., and Saxén, L. (1987). Changes in the glycosylation pattern during embryonic development of mouse kidney as revealed with lectin conjugates. J. Histochem. Cytochem. *35*, 55–65.

Little, M.H. (2006). Regrow or repair: potential regenerative therapies for the kidney. J. Am. Soc. Nephrol. *17*, 2390–2401.

Lustig, B., Jerchow, B., Sachs, M., Weiler, S., Pietsch, T., Karsten, U., van de Wetering, M., Clevers, H., Schlag, P.M., Birchmeier, W., and Behrens, J.

(2002). Negative feedback loop of Wnt signaling through upregulation of conductin/axin2 in colorectal and liver tumors. Mol. Cell. Biol. *22*, 1184–1193.

Maeshima, A., Sakurai, H., and Nigam, S.K. (2006). Adult kidney tubular cell population showing phenotypic plasticity, tubulogenic capacity, and integration capability into developing kidney. J. Am. Soc. Nephrol. *17*, 188–198.

Massengale, M., Wagers, A.J., Vogel, H., and Weissman, I.L. (2005). Hematopoietic cells maintain hematopoietic fates upon entering the brain. J. Exp. Med. *201*, 1579–1589.

Muzumdar, M.D., Tasic, B., Miyamichi, K., Li, L., and Luo, L. (2007). A global double-fluorescent Cre reporter mouse. Genesis *45*, 593–605.

Oliver, J.A., Maarouf, O., Cheema, F.H., Martens, T.P., and Al-Awqati, Q. (2004). The renal papilla is a niche for adult kidney stem cells. J. Clin. Invest. *114*, 795–804.

Ootani, A., Li, X., Sangiorgi, E., Ho, Q.T., Ueno, H., Toda, S., Sugihara, H., Fujimoto, K., Weissman, I.L., Capecchi, M.R., and Kuo, C.J. (2009). Sustained in vitro intestinal epithelial culture within a Wnt-dependent stem cell niche. Nat. Med. *15*, 701–706.

Pleniceanu, O., Harari-Steinberg, O., and Dekel, B. (2010). Concise review: Kidney stem/progenitor cells: differentiate, sort out, or reprogram? Stem Cells *28*, 1649–1660.

Prescott, L.F. (1966). The normal urinary excretion rates of renal tubular cells, leucocytes and red blood cells. Clin. Sci. *31*, 425–435.

Rinkevich, Y., Lindau, P., Ueno, H., Longaker, M.T., and Weissman, I.L. (2011). Germ-layer and lineage-restricted stem/progenitors regenerate the mouse digit tip. Nature *476*, 409–413.

Rinkevich, Y., Mori, T., Sahoo, D., Xu, P.X., Bermingham, J.R., Jr., and Weissman, I.L. (2012). Identification and prospective isolation of a mesothelial precursor lineage giving rise to smooth muscle cells and fibroblasts for mammalian internal organs, and their vasculature. Nat. Cell Biol. *14*, 1251–1260.

Rosenblum, N.D. (2008). Developmental biology of the human kidney. Semin. Fetal Neonatal Med. *13*, 125–132.

Sagrinati, C., Netti, G.S., Mazzinghi, B., Lazzeri, E., Liotta, F., Frosali, F., Ronconi, E., Meini, C., Gacci, M., Squecco, R., et al. (2006). Isolation and characterization of multipotent progenitor cells from the Bowman's capsule of adult human kidneys. J. Am. Soc. Nephrol. *17*, 2443–2456.

Schafer, J.A., Watkins, M.L., Li, L., Herter, P., Haxelmans, S., and Schlatter, E. (1997). A simplified method for isolation of large numbers of defined nephron segments. Am. J. Physiol. *273*, F650–F657.

Singh, S.R., Liu, W., and Hou, S.X. (2007). The adult Drosophila malpighian tubules are maintained by multipotent stem cells. Cell Stem Cell *1*, 191–203.

Spira, E.M., Jacobi, C., Frankenschmidt, A., Pohl, M., and von Schnakenburg, C. (2009). Sonographic long-term study: paediatric growth charts for single kidneys. Arch. Dis. Child. *94*, 693–698.

Ueno, H., and Weissman, I.L. (2006). Clonal analysis of mouse development reveals a polyclonal origin for yolk sac blood islands. Dev. Cell *11*, 519–533.

Valladares Ayerbes, M., Aparicio Gallego, G., Díaz Prado, S., Jiménez Fonseca, P., García Campelo, R., and Antón Aparicio, L.M. (2008). Origin of renal cell carcinomas. Clin. Transl. Oncol. *10*, 697–712.

van Amerongen, R., Bowman, A.N., and Nusse, R. (2012). Developmental stage and time dictate the fate of Wnt/β-catenin-responsive stem cells in the mammary gland. Cell Stem Cell *11*, 387–400.

Wagers, A.J., and Weissman, I.L. (2004). Plasticity of adult stem cells. Cell *116*, 639–648.

Wagers, A.J., Sherwood, R.I., Christensen, J.L., and Weissman, I.L. (2002). Little evidence for developmental plasticity of adult hematopoietic stem cells. Science *297*, 2256–2259.

Witzgall, R., Brown, D., Schwarz, C., and Bonventre, J.V. (1994). Localization of proliferating cell nuclear antigen, vimentin, c-Fos, and clusterin in the postischemic kidney. Evidence for a heterogenous genetic response among nephron segments, and a large pool of mitotically active and dedifferentiated cells. J. Clin. Invest. *93*, 2175–2188.